

Synchronization states and multistability in a ring of periodic oscillators: Experimentally variable coupling delays

Caitlin R. S. Williams,^{1,a)} Francesco Sorrentino,² Thomas E. Murphy,^{3,4} and Rajarshi Roy^{3,5,6}

¹Department of Physics and Engineering, Washington and Lee University, Lexington, Virginia 24450, USA

²Department of Mechanical Engineering, University of New Mexico, Albuquerque, New Mexico 87131, USA

³Institute for Research in Electronics and Applied Physics, University of Maryland, College Park, Maryland 20742, USA

⁴Department of Electrical and Computer Engineering, University of Maryland, College Park, Maryland 20742, USA

⁵Department of Physics, University of Maryland, College Park, Maryland 20742, USA

⁶Institute for Physical Science and Technology, University of Maryland, College Park, Maryland 20742, USA

(Received 12 August 2013; accepted 28 October 2013; published online 11 November 2013)

We experimentally study the complex dynamics of a unidirectionally coupled ring of four identical optoelectronic oscillators. The coupling between these systems is time-delayed in the experiment and can be varied over a wide range of delays. We observe that as the coupling delay is varied, the system may show different synchronization states, including complete isochronal synchrony, cluster synchrony, and two splay-phase states. We analyze the stability of these solutions through a master stability function approach, which we show can be effectively applied to all the different states observed in the experiment. Our analysis supports the experimentally observed multistability in the system. © 2013 AIP Publishing LLC. [<http://dx.doi.org/10.1063/1.4829626>]

Synchronization between delay-coupled oscillators has many applications in biological and technological contexts. In the specific configuration of periodic oscillators connected in a unidirectional ring, changing the coupling time delays can lead to different synchronization relationships between the oscillators. In this paper, we present an experiment of four oscillators coupled in a unidirectional ring, with coupling delays that can be changed to observe different synchronization states.

I. INTRODUCTION

Synchronization between coupled oscillators is of interest to numerous areas of research. In particular, understanding the phase relationship between synchronized oscillators could have applications to coupled neurons in the brain, where synchronization can play a role in neurological disorders. Prasad and his colleagues observed a phase-flip bifurcation, or a transition from in-phase synchrony to out-of-phase synchrony as the coupling delay between two oscillators is increased, both in simulations and in an electronic circuit.¹ Adhikari and his collaborators observed similar transitions for neuron models, including larger numbers of coupled nodes.² There are other examples in nature and applications in technology where the role of synchronization patterns between clock signals is important. For example, specific rhythmic patterns of neural activity generated by groups of neurons which go by the name of *central pattern generators* are known to regulate complex coordinated tasks such as locomotion and respiration.^{3–5}

Previous work has focused on rings of unidirectionally coupled Stuart-Landau oscillators,^{6–8} both in the absence

and in the presence of delays. Choe *et al.* have theoretically considered and numerically simulated systems of delay coupled oscillators, and have shown the ability to control the presence of different synchronization states as the coupling delay is changed.⁹ Other papers have focused on unidirectional rings of coupled chaotic oscillators and found that due to the ring structure, chaos may be suppressed in favor of periodic solutions.^{10–13} Experimental circuitual realizations of unidirectional rings of coupled Lorenz systems were studied in Refs. 11 and 14. However in Refs. 11 and 14, coupling delays were not considered.

Here, we present an experiment of coupled optoelectronic oscillators configured so that the coupling delays can be easily varied. By changing the coupling delays, we observe different synchronization states. The network topology, shown in Fig. 1(a), is composed of four oscillators, each with its own feedback delay τ_f . This feedback creates dynamics in each oscillator, even when they are uncoupled from the other nodes. The four oscillators are delay-coupled together in a unidirectional ring. Each coupling link has delay τ_c , and here we restrict ourselves to the case where $\tau_c \geq \tau_f$. For different values of τ_c , we observe different behaviors of this system, and for some parameter values, we see different behaviors that are dependent on initial conditions, or a multistability of two or more behaviors. We can use a master stability function analysis¹⁵ to evaluate the stability of the observed behaviors.

II. EXPERIMENT

The experimental setup of a single optoelectronic oscillator is shown in Fig. 1(b). In Fig. 1(b), the red lines indicate an optical signal, and the black lines indicate an electronic signal. The coupling delay τ_c is varied by discrete steps by programming the digital signal processing (DSP) board, and τ_f remains fixed. For each measurement, the system always

^{a)}Electronic mail: williamsrsc@gmail.com.

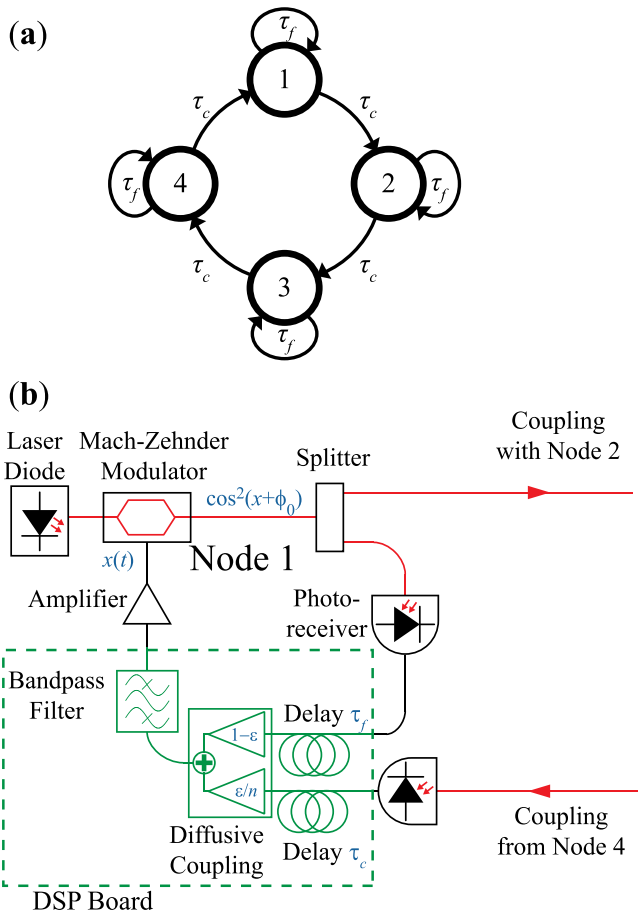


FIG. 1. (a) Schematic of four nodes separated into a unidirectional ring. (b) Experimental setup for a single node, an optoelectronic, nonlinear oscillator, with time-delayed feedback.

starts with both the feedback and coupling disabled, so that only noise is present. Then feedback is enabled, followed by the coupling.

The system is well-modeled by a system of coupled time-delay differential equations:¹⁶

$$\dot{\mathbf{u}}_n(t) = \mathbf{E}\mathbf{u}_n(t) - \mathbf{F}\beta \cos^2(x_n(t - \tau_f) + \phi_0), \quad (1)$$

$$x_n(t) = \mathbf{G} \left\{ \mathbf{u}_n(t) + \epsilon \sum_j K_{nj} [\mathbf{u}_j(t - \tau_c + \tau_f) - \mathbf{u}_n(t)] \right\}, \quad (2)$$

for oscillators $n = 1, \dots, N$, where $x_n \in \mathbb{R}$ are the voltages input to the MZMs and $\mathbf{u}_n \in \mathbb{R}^2$ are the vectors describing the states of the filters. For our ring of four nodes, $N = 4$. The filter is described by constant matrices

$$\mathbf{E} = \begin{pmatrix} -(\omega_H + \omega_L) & -\omega_L \\ \omega_H & 0 \end{pmatrix}, \quad \mathbf{F} = \begin{pmatrix} \omega_L \\ 0 \end{pmatrix}, \quad \text{and } \mathbf{G} = (1 \ 0), \quad (3)$$

and the filter parameters are chosen as $\omega_L = 2\pi \times 2.5$ kHz and $\omega_H = 2\pi \times 0.1$ kHz. The adjacency matrix for a unidirectional ring is given by

$$\mathbf{K} = \begin{pmatrix} 0 & 0 & 0 & 1 \\ 1 & 0 & 0 & 0 \\ 0 & 1 & 0 & 0 \\ 0 & 0 & 1 & 0 \end{pmatrix}. \quad (4)$$

The coupling strength is $\epsilon = 0.2$, the modulator bias is $\phi_0 = \pi/4$, and the feedback strength is $\beta = 1.21$. The feedback delay is fixed at $\tau_f = 1.4$ ms. All parameters are identical for the four nodes. The feedback strength (β) and feedback delay (τ_f) were chosen so that, when uncoupled ($\epsilon = 0$), each node in the network would oscillate periodically.

We vary the value of τ_c and observe the relative phases between the oscillators. As the coupling delay increases from $\tau_c = \tau_f$ we observe in each measurement one of four distinct synchronization states between the four coupled oscillators, as shown in Fig. 2. We can categorize these states by the relative phase δ_k between successive oscillators in synchronization state S_k , $k = 0, \dots, 3$. These states can also be described as *isochronal synchrony* (state S_0 , $\delta_0 = 0$), *splay-phase synchrony*, (state S_1 or state S_3 , $\delta_1 = \pi/2$ or $\delta_3 = 3\pi/2$) and *cluster synchrony* (state S_2 , $\delta_2 = \pi$), which have been described and observed in this and other systems.^{9,17-19} At some values of the coupling delays, bistability is observed between pairs of these synchronization states. For longer coupling delays, we also see multistability between three or all four of these states. Note that in the case of multistability, the phase relationship is determined by the initial conditions, and once the four-node system has established a particular phase relationship after a transient period, the relative phases are maintained. While the time traces shown in Fig. 2 are for the coupled oscillators, they all resemble the time evolution of an uncoupled (isolated) system.

III. STABILITY PREDICTIONS

We also use a master stability function (MSF) approach to evaluate the stability of the system. Previous work using a MSF has focused on the stability of identically synchronous states, though the MSF theory has been extended recently for systems displaying group synchrony.¹⁷⁻¹⁹ Here, we exploit the fact that all the dynamical states displayed in the experiment are periodic and can be written in the following form:

$$\mathbf{u}_n(t) = \mathbf{u}_n(t - T), \quad (5)$$

for $n = 1, 2, 3, 4$ where T is the period of oscillation, which corresponds to the feedback delay of an individual node, τ_f . The different synchronous solutions can be written as

$$\mathbf{u}_n(t) = \mathbf{u}_{n-1} \left(t - \frac{\delta_k}{2\pi} T \right), \quad n = 2, 3, 4, \quad (6a)$$

$$\mathbf{u}_1(t) = \mathbf{u}_4 \left(t - \frac{\delta_k}{2\pi} T \right). \quad (6b)$$

Similar periodic patterns, called *rotating waves*, have also been observed when chaotic oscillators are coupled in a unidirectional ring.^{10,11,13}

The adjacency matrix has eigenvalues $\{\lambda_m = (i)^m\}$ (i is the imaginary unit) and eigenvectors $\ell_m (\mathbf{K}\ell_m = \lambda_m \ell_m)$, $m = 0, \dots, 3$. Moreover, each observed state S_k corresponds to the eigenvector ℓ_k , $k = 0, \dots, 3$. In order for state S_k to be stable, perturbations orthogonal to ℓ_k must be decaying.

To evaluate the stability of a given synchronous state, we take Eqs. (1) and (2) with the specific coupling matrix,

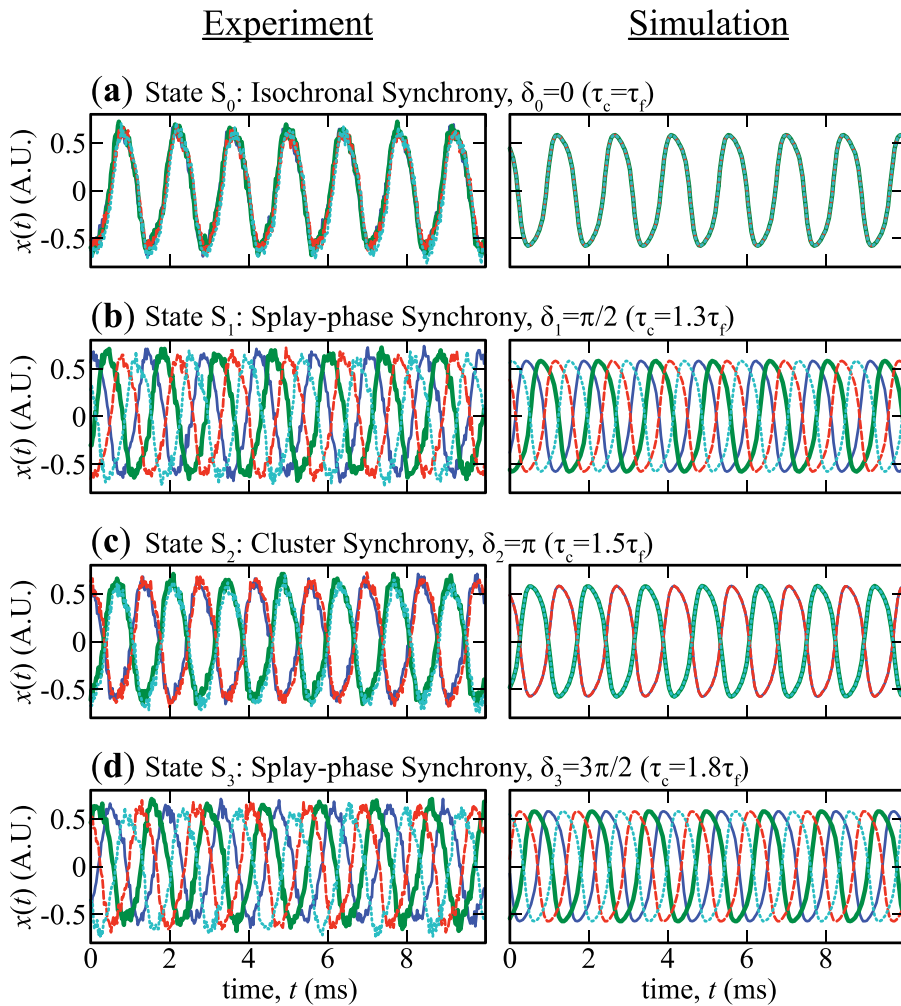


FIG. 2. Representative time traces for four different values of the coupling delay, each displaying a different phase relationship between the four nodes, as denoted by δ_k , the phase shift between successive oscillators in state S_k . Experimental traces are on the left; simulations are on the right.

Eq. (4), and linearize about a given synchronous solution (6), obtaining,

$$\begin{aligned} \Delta \dot{\mathbf{u}}_n &= \mathbf{E} \Delta \mathbf{u}_n + \mathbf{F} \beta \sin(2\mathbf{G} \epsilon \mathbf{u}_{n-1}(t - \tau_c) + 2\phi_0) \\ &\times \mathbf{G} \epsilon \sum_j K_{nj} \Delta \mathbf{u}_j(t - \tau_c), \end{aligned} \quad (7)$$

$n = 1, \dots, 4$ and $\mathbf{u}_{n-1} = \mathbf{u}_4$ for $n = 1$. We note that, by virtue of Eq. (6), $\mathbf{u}_{n-1}(t - \tau_c) = \mathbf{u}_n(t + [\delta_k/2\pi]T - \tau_c)$, $n = 2, \dots, 4$ and $\mathbf{u}_4(t - \tau_c) = \mathbf{u}_1(t + [\delta_k/2\pi]T - \tau_c)$. By using the ansatz $\Delta \mathbf{u}_n(t) = c_n \mathbf{v}(t)$, we obtain the result that stability is governed by the following low-dimensional equation:

$$\begin{aligned} \dot{\mathbf{v}} &= \mathbf{E} \mathbf{v} + \mathbf{F} \beta \sin\left(2\mathbf{G} \epsilon \mathbf{u}_n\left(t + \frac{\delta_k}{2\pi}T - \tau_c\right) + 2\phi_0\right) \\ &\times \mathbf{G} \epsilon \lambda_m \mathbf{v}(t - \tau_c). \end{aligned} \quad (8)$$

Now in order to evaluate stability, we would need to compute the Lyapunov exponents associated with Eq. (8). The maximum Lyapunov exponent (MLE) for a particular value of τ_c is the MSF. A negative MLE indicates that the particular synchronization state under consideration will be stable. Note that Eq. (8) still depends on the node index $n = 1, \dots, 4$ through the driving term $\mathbf{u}_n(t + [\delta/2\pi]T - \tau_c)$. However, the synchronous solutions $\{u_n\}$ are identical, apart from a temporal shift, as given in Eq. (6). Therefore, the choice of the

specific n is irrelevant for determination of the Lyapunov exponents, which are asymptotically defined quantities, and any oscillator n can be arbitrarily chosen to drive Eq. (8).

For each synchronization state S_k , we insert the appropriate δ_k into Eq. (8), and evaluate Eq. (8) for all $m = 0, \dots, 3$, excluding $m = k$ from our calculation of the MLE because we are interested only in perturbations orthogonal to ℓ_k for the stability of state S_k . For the isochronal synchrony case (S_0), the eigenvector corresponding to the synchronous state is $\ell_0 = [1, 1, 1, 1]$, so we ignore the Lyapunov exponent corresponding to the eigenvalue $\lambda_0 = 1$ when calculating the MSF. For the splay-phase synchronous states (S_1, S_3), the eigenvectors corresponding to these synchronous states are $\ell_1 = [1, i, -1, -i]$ or $\ell_3 = [1, -i, 1, i]$, so the ignored eigenvalues are $\lambda_1 = i$ and $\lambda_3 = -i$, respectively. For the cluster synchrony state (S_2), the corresponding eigenvector and ignored eigenvalue are $\ell_2 = [1, -1, 1, -1]$ and $\lambda_2 = -1$.

The stability results for each of the four synchronization states as a function of τ_c are shown in Fig. 3. For the smaller values of τ_c , only one or two of the states are stable for a particular value of τ_c . However, as τ_c increases, there are windows of multistability where three or four states are stable.

IV. RESULTS AND DISCUSSION

For each coupling delay $1.4 \text{ ms} < \tau_c < 3 \text{ ms}$, we performed 10 independent experiments and 2000 simulations,

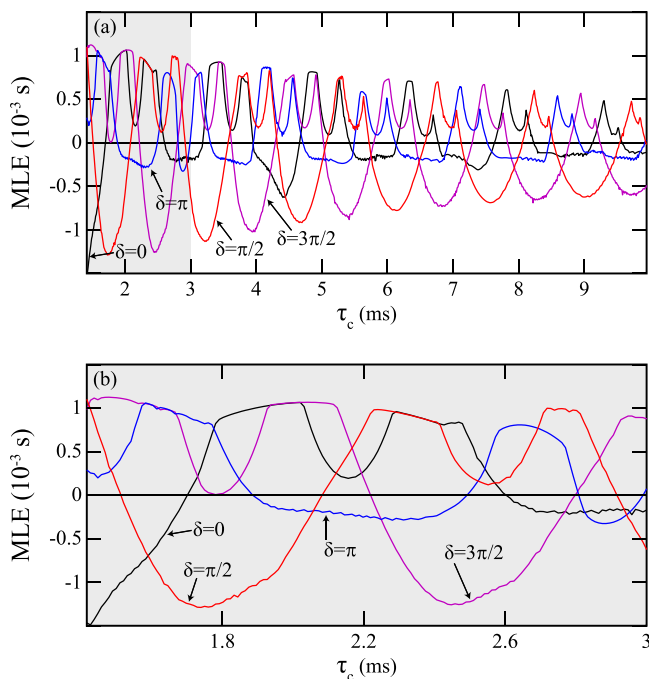


FIG. 3. Master stability function, or maximum Lyapunov exponent (MLE), of four different synchronization states: $\delta_0=0$ (isochronal synchrony), $\delta_1=\pi/2$ or $\delta_3=3\pi/2$ (splay-phase synchrony), and $\delta_2=\pi$ (cluster synchrony). A negative MLE indicates the stability of a particular phase relationship. (a) MLE as a function of coupling delay τ_c calculated over a wide range of delays. (b) Enlargement of (a) for narrow range of τ_c .

each starting from random initial conditions and observed how frequently each synchronization state occurred. The results are shown in Fig. 4. As the time delay τ_c is increased, the observed phase lag δ between successive oscillators increases in a step-like manner, separated by regions of bistability in which the system could fall into one of two possible stable synchronization patterns. For the coupling delay range shown in this figure, only one or two different phase relationships were observed for each value of the coupling delay, with good agreement between experiment and simulation. For the values of τ_c for which a particular phase relationship synchronization state has a negative MLE, we see the corresponding synchronization state displayed in simulation and experiment. If, for a particular value of τ_c , more than one phase relationship is stable, we see the corresponding two or three synchronization states in simulation and experiment. The particular state that is present depends on the initial conditions.

For longer coupling delays, near $\tau_c=8$ ms, the results from simulations are shown in Fig. 5, where there can be three different relationships shown, as we expect from the MSF calculations shown in Fig. 3(a). In the experiment, we also observe multistability between three synchronization states for larger values of τ_c . We note that increasing the coupling delay increases the overlapping areas of stability.

A comparison of Figs. 3(b) and 4 show good agreement between simulation, experiment, and calculated stability. The observations of particular phase relationships in experiment and simulation correspond well to the regions where the MSF analysis predicts stability for those different phase relationships.

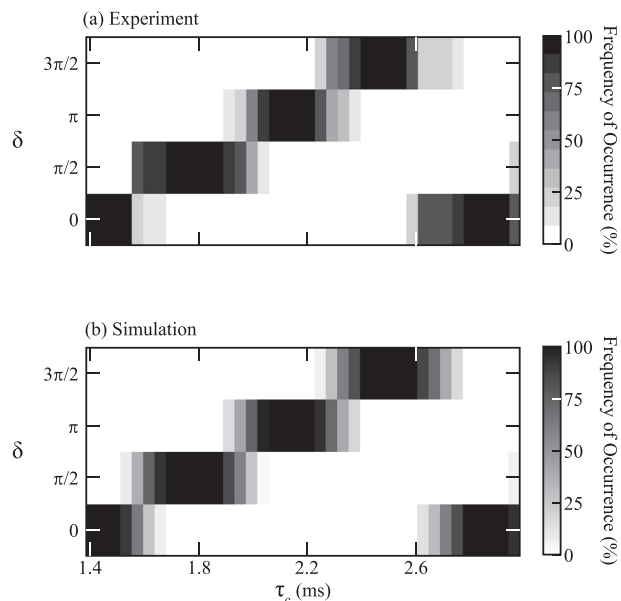


FIG. 4. The phase relationships present as a function of coupling delay. For each coupling delay τ_c , the percentage of different random initial conditions resulting in a particular phase relationship δ is shown by the grayscale. The top figure shows the experimental results, with 10 different initial conditions for each delay. The bottom figure shows the simulations results, with 2000 different initial conditions for each delay.

We have observed a transition from in-phase, isochronal synchrony to splay-phase synchrony as we change the coupling delay to values larger than the internal delay. We have further observed three additional transitions—splay-phase \rightarrow cluster, cluster \rightarrow splay-phase, splay-phase \rightarrow isochronal—as the coupling delay is increased to twice the feedback delay, and the transitions appear to be cyclic as the coupling delay is further increased. The transitions are not sharp; for intermediate ranges of coupling delays, bistability is sometimes observed. This phenomenon was also observed in simulations of a unidirectional ring of coupled Stuart-Landau oscillators.⁹

While multiple patterns of synchronization can occur in a unidirectional ring with symmetric coupling, real systems may have asymmetric or inhomogeneous delays between elements. The propagation time for a signal in the nervous system, for example, can be different for each link. Two recent papers describe different synchronization patterns that occur in a unidirectional ring of oscillators or modeled

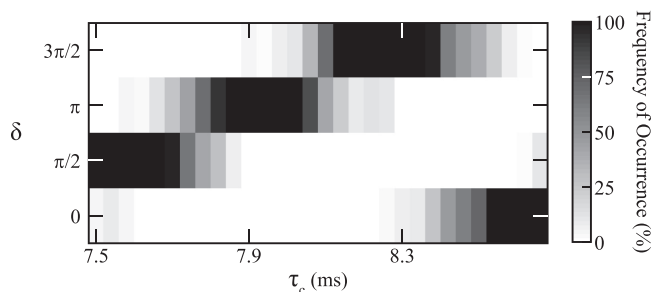


FIG. 5. Multistability between synchronization states for long coupling delays, as observed for 50 different random initial conditions in simulations.

neurons, both for homogeneous delays and for inhomogeneous delays.^{8,20} By changing the coupling delays so that they are not all equal, a variety of synchronization states can be created, and the state is determined by the values of the coupling delays.

While our investigation focused on the case of four equal coupling delays, we also experimentally and numerically investigated the case where the coupling delays are not identical, but the sum of the four coupling delays is held constant. In this investigation, we focused on the case where the average coupling delay corresponds to the value of τ_c for which isochronal synchrony is stable in the case of four equal coupling delays. In this case, we can write the solutions as time-shifted copies of each other, with time shifts that correspond to the differences between the coupling delays. Because the nodes are connected sequentially and each node acts as a time-invariant oscillator, a node followed by a delay is indistinguishable from a node preceding delay when viewed from the perspective of the remainder of the system. Synchronization patterns for non-identical coupling delays constitute an interesting problem for future study.

V. CONCLUSION

In conclusion, we have presented an experiment of four optoelectronic oscillators coupled in a unidirectional ring, in which the coupling delays can be varied. We have observed four different synchronization states as the coupling delay is varied, including isochronal synchrony, cluster synchrony, and splay-phase synchrony. We have compared our experimental results with simulations and numerical stability computations using a master stability function approach.

ACKNOWLEDGMENTS

The authors would like to thank Ulrike Feudel for helpful discussions. This work was supported by DOD MURI grant ONR N000140710734.

- ¹A. Prasad, S. K. Dana, R. Karnatak, J. Kurths, B. Blasius, and R. Ramaswamy, *Chaos* **18**, 023111 (2008).
- ²B. M. Adhikari, A. Prasad, and M. Dhamala, *Chaos* **21**, 023116 (2011).
- ³J. Murray, *Mathematical Biology: I. An Introduction, Interdisciplinary Applied Mathematics* (Springer, 2002) Chap. 12.
- ⁴A. Cohen, P. Holmes, and R. Rand, *J. Math. Biol.* **13**, 345 (1982).
- ⁵C. von Euler, *J. Appl. Physiol.* **55**, 1647 (1983).
- ⁶S. Yanchuk and M. Wolfrum, *Phys. Rev. E* **77**, 026212 (2008).
- ⁷P. Perlikowski, S. Yanchuk, O. Popovych, and P. Tass, *Phys. Rev. E* **82**, 036208 (2010).
- ⁸O. V. Popovych, S. Yanchuk, and P. A. Tass, *Phys. Rev. Lett.* **107**, 228102 (2011).
- ⁹C.-U. Choe, T. Dahms, P. Hövel, and E. Schöll, *Phys. Rev. E* **81**, 025205 (2010).
- ¹⁰M. Matías, J. Güémez, V. Pérez-Munuzuri, I. Marino, M. Lorenzo, and V. Pérez-Villar, *Europhys. Lett.* **37**, 379 (1997).
- ¹¹M. Matias, V. Pérez-Munuzuri, M. Lorenzo, I. Marino, and V. Pérez-Villar, *Phys. Rev. Lett.* **78**, 219 (1997).
- ¹²M. Matías and J. Güémez, *Phys. Rev. Lett.* **81**, 4124 (1998).
- ¹³X. Deng and H. Huang, *Phys. Rev. E* **65**, 055202 (2002).
- ¹⁴E. Sánchez and M. Matías, *Phys. Rev. E* **57**, 6184 (1998).
- ¹⁵L. M. Pecora and T. L. Carroll, *Phys. Rev. Lett.* **80**, 2109 (1998).
- ¹⁶T. E. Murphy, A. B. Cohen, B. Ravoori, K. R. B. Schmitt, A. V. Setty, F. Sorrentino, C. R. S. Williams, E. Ott, and R. Roy, *Phil. Trans. R. Soc. A* **368**, 343 (2010).
- ¹⁷F. Sorrentino and E. Ott, *Phys. Rev. E* **76**, 056114 (2007).
- ¹⁸T. Dahms, J. Lehnert, and E. Schöll, *Phys. Rev. E* **86**, 016202 (2012).
- ¹⁹C. R. S. Williams, T. E. Murphy, R. Roy, F. Sorrentino, T. Dahms, and E. Schöll, *Phys. Rev. Lett.* **110**, 064104 (2013).
- ²⁰S. Yanchuk, P. Perlikowski, O. V. Popovych, and P. A. Tass, *Chaos* **21**, 047511 (2011).